

**Seismicity associated with the 1991–1995 dome growth  
at Unzen Volcano, Japan**

**K. Umakoshi<sup>a,\*</sup>, N. Takamura<sup>a</sup>, N. Shinzato<sup>a</sup>,  
K. Uchida<sup>b</sup>, N. Matsuwo<sup>b</sup>, H. Shimizu<sup>b</sup>**

*<sup>a</sup>Faculty of Environmental Studies, Nagasaki University, 1-14 Bunkyo-machi,  
Nagasaki 852-8521, Japan*

*<sup>b</sup>Institute of Seismology and Volcanology, Faculty of Sciences, Kyushu University,  
2-5643-29 Shin-yama, Shimabara, Nagasaki 855-0843, Japan*

\* Corresponding author. Tel./fax: +81-95-819-2766

*E-mail address:* umakoshi@nagasaki-u.ac.jp (K. Umakoshi)

Submitted to Journal of Volcanology and Geothermal Research

## **Abstract**

From May 1991 until February 1995, seismicity in the crater area of Unzen Volcano, southwest Japan, intensified in conjunction with the growth of a dacite lava dome. We used data from seismic stations located near the crater to identify approximately 580,000 summit earthquakes with maximum amplitudes equal to or greater than  $1 \times 10^{-3}$  cm/s. The temporal characteristics of the seismicity level were different for exogenous and endogenous periods of dome growth. Periods of solely exogenous growth were accompanied by several days or weeks of increased seismicity, and levels of seismicity were notably reduced between successive seismically active periods. In contrast, levels of seismicity were generally high during periods when the dome grew endogenously, with repeated cycles of increasing and decreasing seismicity of one to two months duration. We classified the waveforms of summit earthquakes into high-frequency (HF), medium-frequency (MF), and low-frequency (LF) types on the basis of spectral analysis. Dominant waveform types varied significantly over time: HF was dominant in May 1991, LF from June 1991 until August 1993, MF during September and October 1993, and HF and MF from November 1993. HF and MF events are mainly distributed at depths of 500–1100 m above sea level (ASL), just below the lava dome, while LF events are widely distributed at depths from 500 m ASL to the interior of the dome itself. To efficiently detect earthquake families, we conducted a cross-correlation analysis of waveforms. Using the events one-by-one as reference events, we calculated peak correlation coefficients between each reference event and events that occurred within 24 h either side of the reference event. The results show that many earthquake families of all waveform types occurred throughout the growth period of the dome. The durations of most families were less than two weeks and were not related to the intensity of seismic activity. The incidence

rate of events within each family reached a peak in the middle of the respective activity period. The results also suggest that the waveforms in several analyzed families gradually evolved over time. During periods when HF events intensified, several families appeared contemporaneously. In contrast, during periods when LF events intensified, the occurrence pattern of earthquake families was relatively simple: a new family became active only once the activity of the previous family had declined or ceased completely. A possible source mechanism for families of HF events is stick-slip within the stiff rocks surrounding the conduit; however, several different types of source mechanisms should be considered for families of LF events.

Keywords: seismicity; cross-correlation; earthquake families; lava dome; Unzen

## 1. Introduction

Fugendake, the main peak of Unzen Volcano, southwest Japan, began to erupt on November 17, 1990, and growth of an associated dacite lava dome occurred from May 20, 1991 until early February 1995. Soon after the eruption began, seismic observations were reinforced (Geophysical Party, Joint University Research Group, 1992; Shimizu et al., 1992b) and large amounts of seismic data were obtained. Seismic signals recorded at the volcano have their origin in volcano-tectonic (VT) earthquakes, summit earthquakes, volcanic tremors, a Vulcanian eruption, pyroclastic flows, and debris flows. Fig. 1 shows the hypocentral distribution of VT and summit earthquakes, as determined by Umakoshi et al. (2001) and the Shimabara Earthquake and Volcano Observatory (now known as the Institute of Seismology and Volcanology) of Kyushu University (SEVO). VT seismicity was active mainly on the western side of the volcano during the period from one year prior to the eruption to the initiation of dome extrusion. In contrast, summit earthquakes, which are volcanic earthquakes that occur at shallow depths in the crater area, intensified from the time immediately prior to dome emergence until the cessation of dome growth. The hypocentral area of summit earthquakes is separated from that of VT earthquakes by an aseismic area within approximately 4 km to the west of the lava dome.

Seismic monitoring during the eruption reveals that the level of summit seismicity changed significantly over the period of dome growth (e.g., Nakada et al., 1999). For example, the number of summit earthquakes increased markedly immediately prior to the onset of the extrusion of the lava lobe from a new vent. One of the most conspicuous features of summit seismicity was the occurrence of earthquake families: earthquake groups with similar waveforms (Okada et al., 1981). Sudo et al. (1992; 1994) detected numerous families during periods of lobe growth. The Japan Meteorological Agency (JMA; 2002) reported that earthquake families occurred during

periods of both endogenous and exogenous dome growth. Umakoshi et al. (2002) investigated the waveforms of summit earthquakes from November 1993 until January 1994 and detected many earthquake groups in which waveforms evolved slightly over time. They demonstrated that the activity of some groups was linked to ground deformation on the upper southern flank of the volcano.

Thus, summit seismicity is closely related to dome activity; however, the detailed characteristics of summit seismicity are not yet completely understood because seismic data recorded at stations located near the dome have yet to be consistently analyzed for the entire period of dome growth. Accordingly, the current paper presents an analysis of overall summit seismicity from May 1991 until February 1995 using data from seismic stations located near the dome.

## **2. 1991–1995 dome growth at Unzen Volcano**

During lava effusion over a period of about three years and nine months, thirteen discrete lobes formed by exogenous growth; these are designated Lobes 1–13 (Ohta, 1997). The dome also commonly exhibited endogenous growth that occurred when new magma intruded into the dome without new lava being extruded to the surface. Fig. 2 shows the daily effusion rate of lava over the study period (Nakada et al., 1999). Ohta (1997) divided the 1991–1995 period of dome growth into three stages on the basis of temporal changes in the dominant growth style of the lava dome (see upper Fig. 2). Lobes 1–9 grew during Stage 1, and concurrent endogenous growth was observed from late November 1991 to December 1992. Stage 2 corresponds to the first half of the second pulse of lava effusion, when exogenous growth was vigorous and Lobes 10 and 11 developed. In Stage 3, the dominant growth style changed to endogenous growth, although small, short-lived lobes emerged (Lobes 12 and 13). From October 1994, a lava spine began upheaving immediately above the previous Jigokuato crater, from

where Lobe 1 had extruded. The upheaval had ceased by February 1995, and the eruption ended. The total volume of extruded lava is estimated to be  $2.1 \times 10^8 \text{ m}^3$  (Nakada et al., 1999), and the new lava dome was named “Heisei-Shinzan” in 1996 (Fig. 3). The previous Jigokuato crater was located at an altitude of about 1250 m, just below the peak of “Heisei-Shinzan.”

### 3. Data and methods

Seismic data used in this study were obtained by SEVO (Shimizu et al., 1992b). Fig. 3 shows the locations of seismograph stations close to the dome that were installed prior to emergence of the dome on May 20, 1991. Note that the seismometer at FG3 was moved to the location at FG4 during June 1993. All stations were equipped with 1-Hz vertical-component seismometers. Signals were telemetered to SEVO and recorded continuously on digital audiotapes with a sampling rate of 100 Hz. The frequency characteristic of the overall observation system is nearly flat for velocities between 1 and 20 Hz. During the study period, data from FG3 and FG4 were successfully acquired at a rate of about 95%, which is superior to the rate for FG1. There were also a number of very small events that were clearly recorded only at FG3 or FG4. For these reasons, we mainly analyzed waveform data from FG3 and FG4.

We consider that those events detected only at FG3 or FG4, as well as events with the earliest arrival time of seismic wave recorded at FG1, FG3, or FG4, to be summit earthquakes. Although volcanic tremors and “avalanche” earthquakes (Zobin et al., 2005) generated by pyroclastic flows and rockfalls also meet these criteria, they were excluded from the analysis. As these excluded events were generally of longer duration than summit earthquakes, we were able to recognize most of them by visual inspection of waveforms. To create a data set of P-wave arrival times, we used a method that combined automatic and manual processes. This involved automatic event-detection

based on average absolute amplitudes at 0.1 s intervals, the removal of events except summit earthquakes by visual inspection of waveforms, and the manual revision of arrival times for those cases with errors of more than 1 s.

Although Nakada et al. (1999) classified summit earthquakes as HF (predominant frequency, 5–10 Hz) and LF (1–5 Hz) types, we reclassified them as HF (>7 Hz), MF (4–7 Hz), and LF (1–4 Hz) types. Having calculated the spectra of waveforms by FFT with a window length of 5.12 s from 0.5 s before onset, we then automatically classified the earthquakes by comparing the summations of spectral amplitude in each range. Fig. 4 shows examples of waveforms and spectra for each earthquake type.

To efficiently detect earthquake families, we conducted a cross-correlation analysis of waveforms using the following method. Using every event one-by-one as reference events, we calculated peak cross-correlation coefficients (PCCs) between each reference event and events that occurred within 24 h either side of the reference event. A PCC is defined as the maximum value among cross-correlation coefficients obtained by fixing the reference waveform and varying the other waveform within a range of  $\pm 2$  s. We used a correlation window length of 5.5 s starting 0.5 s prior to the onset of the event. For each reference event, we counted the number of events with PCCs equal to or greater than a given threshold value; a PCC threshold of 0.6 was chosen for the present analysis, as explained in Section 4.2.

## 4. Results

### 4.1 Seismicity

We identified approximately 580,000 events whose maximum amplitudes are equal to or more than  $1.0 \times 10^{-3}$  cm/s. The noise level was generally less than  $3 \times 10^{-4}$  cm/s, but seismograms were occasionally disturbed (mainly due to “avalanche” earthquakes), resulting in poor event identification. We have yet to estimate the magnitudes for all

events because the waveforms recorded at FG3 and FG4 were saturated for approximately 11% of the events. According to JMA (2002), the maximum magnitude for summit earthquakes is 2.9, which occurred in December 1993 and January 1994. The minimum magnitude is estimated to be about  $-2.0$ , which was obtained using waveform data recorded at FG2 (Umakoshi et al., 2002). Fig. 5(c) shows the daily number of earthquakes, with the lengths of red, green, and blue bars corresponding to the numbers of HF, MF, and LF events, respectively. The results show that both the seismicity level and dominant waveform type varied markedly over the study period. Based on the temporal characteristics of seismicity and waveform types, we subdivided each of the three stages shown in Fig. 2 into two or three sub-stages, as indicated in Fig. 5(b) and Table 1. Fig. 5(a) shows the growth style of the lava dome over time. The nature of seismicity and associated dome activity during each sub-stage are as follows.

Stage 1–1. A gradual increase in summit seismicity was recorded from May 12, 1991, approximately one week before the dome (Lobe 1) emerged, Inflation on the upper southern flank of the volcanic edifice was observed by electron-optical distance measurements (Saito et al., 1993). Following emergence of the dome, both seismicity and the rate of inflation gradually decreased. During this sub-stage, 58% of the events were of HF type.

Stage 1–2. During this sub-stage, only exogenous dome growth was observed, and Lobes 2–4 emerged. The activity of HF events declined and the proportion of LF events increased. The main peaks in August and September coincide with the births of Lobes 3 and 4, respectively. During the periods that these lobes were growing, the level of seismicity was notably reduced.

Stage 1–3. Lobes 5–9 were extruded, and simultaneous dome growth occurred endogenously in the vicinity of the vent of Lobe 5, about 300 m east of Jigokuato crater. The seismicity level of LF events was generally high. Following the emergence of Lobe

9, the level of seismicity gradually decreased and lava effusion declined to a rate of less than  $1.0 \times 10^5 \text{ m}^3/\text{day}$  (Fig. 2).

Stage 2–1. Dome growth was dominantly exogenous and Lobes 10 and 11 were extruded. The proportions of different event types were almost the same as recorded in Stage 1–3. Periods of increased seismicity before March 1993 were recorded at the times that each of the lobes began to extrude. From late July to early August 1993, the number of LF events reached a maximum. A total of 8042 events were recorded on July 31; the greatest number of events was recorded during dome growth, but the maximum amplitudes of these events were generally smaller than those of LF events during other periods.

Stage 2–2. Lobe 11 had grown to a length of 750 m by the end of September 1993 (JMA, 2002), but its rate of growth was declining. The dominant waveform of summit earthquakes changed to MF type.

Stage 3–1. HF events increased in number during this period and the level of seismicity was generally high. MF events were also commonly observed, but few LF events were recorded. Vigorous endogenous dome growth was observed, with occasional ground deformation on the upper flank of the volcanic edifice (Suto et al., 1994; JMA, 2002). Lobes 12 and 13 began to grow during January and July 1994, respectively, but they only grew for periods of several weeks.

Stage 3–2. A lava spine began to upheave at the top of the endogenous dome. Seismic activity was markedly reduced, but periodic increases in HF events were observed synchronous with tilt oscillation on the volcanic edifice (Yamashina et al., 1999). The periodicity continued until January 1995, and seismicity began to gradually decrease.

## 4.2 Earthquake families

To explain our choice of threshold PCC value, we first present the results of cross-correlation analysis for the period May 15 to June 15, 1994 (Fig. 6). The horizontal axis represents the occurrence time of reference events, while the vertical axis is the number of events with a PCC equal to or greater than the threshold value within 24 h either side of the reference event. Figs. 6 (a) to (f) shows results for different PCC threshold values. PCC threshold values of 0.6 and 0.7 yield the greatest concentration of data, indicating that these values result in the most successful classification of events. Similar results were obtained for other time periods. As no marked differences are evident between the results for thresholds of 0.6 and 0.7, we use the data for a threshold of 0.6 in the following analysis.

Fig. 5(d) shows the number of events with a PCC equal to or greater than 0.6 within 24 h either side of the reference event. A large number of peaks are apparent, each of which indicates the occurrence of an earthquake family or group. We use the term “Earthquake group” to represent a group of events whose waveforms vary slightly over time (Umakoshi et al., 2002); however, as we have yet to investigate temporal changes in waveforms within each group, hereafter we use the term “earthquake family” for all detected groups. We identified at least 50 families in Fig. 5(d) with peak values in excess of 500, with much greater numbers of smaller families. An arch-like distribution of data was typically observed, which indicates that the incidence rate of events within a family gradually increased and then decreased over time. We approximated the duration of each family by measuring the base widths of each arch-like distribution of data. The duration of most families was less than two weeks, which appears to be unrelated to the peak values evident in Fig. 5(d). Fig. 7 shows the waveforms of families observed during each month, as represented by the events with the highest peaks in Fig. 5(d).

Fig. 8 shows an enlargement of part of Fig. 5(d) for four periods, demonstrating two typical occurrence patterns of families. In May 1991 and May–June 1994, several families appeared contemporaneously (TYPE I). In contrast, in December 1991 and July–August 1993, the occurrence pattern of families was relatively simple: new earthquake families only began to emerge once the activity of the previous family had declined or ceased completely (TYPE II). TYPE I activity was mainly observed during Stages 1–1 and 3–1, with TYPE II activity observed during Stages 1–2, 1–3, 2–1, and 2–2. The occurrences of families with TYPE I and TYPE II correspond to periods of increased HF and LF events, respectively.

## 5. Discussion

On the basis of the temporal data shown in Fig. 5(c), we identify two types of seismicity patterns. First, in Stages 1–2 and 2–1, seismicity intensified for several days or weeks at a time and was notably low between successive seismically active periods. Second, in Stages 1–3 and 3–1, the seismicity level was generally high, with repeated cycles of increasing and decreasing seismicity over periods of one to two months. The former and latter types of seismicity patterns coincide with periods of exclusively exogenously dome growth and periods when the dome grew endogenously or both exogenously and endogenously, respectively. This suggests that the two types of seismicity patterns are related to the style of growth of the lava dome, especially in terms of whether endogenous growth occurred.

During periods of exogenous growth, several peaks in seismicity level correspond with the times that new lobes appeared. Shimizu et al. (1997) proposed that the increased seismicity at these times reflected the fracturing of rock associated with the formation of a new vent, as epicenters were concentrated in the vicinity of the vent. We are also confident that the periods of low seismicity reflect the smooth aseismic

extrusion of lava to the surface. In contrast, during periods of endogenous growth, lava was unable to extrude to the surface; this resulted in increased magmatic pressure within the dome and the conduit and increased pore pressure in the surrounding rock, producing high levels of seismicity.

The dominant waveform types of summit earthquakes over the period of dome growth changed sequentially from LF to HF and MF types, except for a period of increased HF events in May 1991. To investigate differences in the locations of hypocenters for the different event types, we divided the hypocenters shown in Fig. 1(c) in terms of the three event types. Fig. 9 shows the hypocentral distribution for each event type. These hypocenters were obtained via the master event method using data from six seismic stations (Fig. 10) (Shimizu et al., 1994). The one-dimensional velocity structure used in this method was based on the results of air-gun experiments (Urabe et al., 1987) and a simple experiment at a site adjacent to the lava dome to determine the P-wave velocity near the surface (Shimizu et al., 1992a). Accordingly, we consider that both the relative and absolute locations of hypocenters are sufficiently reliable to enable a discussion of their spatial distribution. As the hypocentral areas for different event types overlap in part, differences in the recorded waveform types cannot be explained solely on the basis of path effects: the differences probably also reflect source effects.

The epicenters of HF and MF events are distributed near the previous Jigokuato crater, just below the peak of “Heisei-Shinzan” (Fig. 3), while the epicentral area of LF events is relatively widely spread, mainly extending to the east. This distribution is probably related to the fact that the vents of Lobes 2–13 opened within 300 m to the east of Jigokuato crater. The hypocentral depths of HF and MF events are mainly distributed within 500–1100 m above sea level (ASL), while those of LF events are widely distributed from 500 m ASL to the interior of the lava dome itself. Although the

events shown in Fig. 9 only represents about 2% of the total number of events detected in this study, they suggest that the upper limit of hypocentral depths of HF and MF events is deeper than that of LF events. This inference is supported by the fact that ground deformation on the upper flank of the volcanic edifice was commonly observed during periods of intensive HF events (Saito et al., 1993; Suto et al., 1994; JMA, 2002) and that infrasonic pulses accompanied by weak gas emission from the dome surface were only observed at the times of LF events (Yamasato, 1998). The resumption of HF events during Stage 3–1 may indicate an increase in magmatic pressure within the conduit. The increase in pressure probably developed because the dome was so large that it inhibited the ascent of magma within the conduit.

The appearance of earthquake families is considered to be a common feature of seismicity associated with the emplacement of lava domes (Power et al., 1994; White et al., 1998). During the 1991–1995 dome growth at Unzen, a large number of earthquake families appeared at all stages of growth. Also, the families were recorded with all three waveform types. The characteristics of the families have not been investigated in detail except for those that occurred in the period November 1993 to January 1994 (Umakoshi et al., 2002). In the present study, we analyzed four new families, F1–F4, as shown in Fig. 8. F1 and F2 are HF and MF event families, respectively, while F3 and F4 are both LF event families. We used a method developed by Umakoshi et al. (2002) to extract events belonging to each family. Those events that show peak values in Fig. 8 were used as master events; their waveforms are shown in Fig. 7. According to this method, events whose waveforms vary slightly over time are also considered to be a family; accordingly, all pairs of events within a family do not always have PCCs equal to or greater than the threshold value, and it is possible that waveforms within a family change significantly over the duration of the activity. The extracted events for each family are shown by red dots in Fig. 8. Fig. 11 shows PCCs between the master

event and all extracted events (a), the number of events recorded in 3-hour intervals (b), and the maximum amplitude measured in digital counts (c) for families F1–F4. The PCCs in F1 (Fig. 11, F1(a)) do not always give true values because the waveforms from FG3 were saturated for many events. For the same reason, data from FG2 were used in compiling F1 (Fig. 11, F1(c)).

We note the following characteristics of the activities of the different families. First, temporal changes in the upper limits of PCCs gradually decreased either side of the master event for F1, F2, and F4; this suggests that the waveforms evolved gradually over time. This characteristic has also been observed at Usu Volcano, Japan (Mizukoshi and Moriya, 1980) and Redoubt Volcano, Alaska (Stephens and Chouet, 2001). In contrast, Green and Neuberg (2006) demonstrated that there was no pattern of evolution in the LF event families that occurred at Soufriere Hills Volcano, Montserrat, during June 1997. We consider that a gradual evolution of waveforms is generated by not only the progressive migration of hypocenters and/or gradual changes in source mechanisms but also changes in the structure of the source region such as the progress of fractures associated with deformation of the volcanic edifice. Second, the number of events recorded in 3-hour intervals (incidence rate of events) culminated in the middle part of the activity period for all four families. The occurrence of numerous arch-like distributions of data in Fig. 5(d) suggests that many other families also share this characteristic. Third, the upper limit of amplitude changes smoothly over time in F1 ad F4, although we are unable to consider the lower limit of amplitude because of the restriction of event selection on the amplitude of waveforms. Fourth, the duration of families does not show a correlation with either the maximum incidence rate of events or the total number of events. For example, the duration of F4 is shorter than that of F2, even though activity of F4 was much more intense. As stated in Section 4.2, the duration of most families was less than two weeks, regardless of the

peak values shown in Fig. 5(d). These observations indicate that the durations of families were not related to the intensity of seismic activity. The four characteristics described above have also been recognized in many HF event families that occurred between November 1993 and January 1994 (Umakoshi et al., 2002).

It is difficult for us to investigate the source process of summit earthquakes in detail because of the low dynamic range and narrow band observation system used in our analysis; however, previous studies have used the polarization of P-wave first motions to analyze focal mechanisms for a number of relatively large earthquakes. Shimizu et al. (1994) analyzed HF events that occurred immediately prior to dome emergence on May 1991 (Stage 1–1) and obtained solutions of normal faulting. We consider that the HF events recorded during Stage 1–1 occurred in the stiff rocks surrounding the conduit following the development of excessive magmatic pressure. The simultaneous occurrence of several different families (TYPE I described in Section 4.2) indicates that stick-slip events occurred concurrently at different locations around the conduit. The generation process of HF and MF event families during Stage 3–1 may well be the same as that for Stage 1–1, as the same occurrence pattern of families was observed for both Stage 3–1 and Stage 1–1. Shimizu et al. (1992s) also analyzed the hypocentral locations and focal mechanisms of LF events that occurred during September 1992. Their results indicate that the hypocenters were concentrated at the site of marked dome deformation and that the focal mechanism can be explained by the double-couple force. They also concluded that the analyzed LF events were generated by stick-slip between solidified lava blocks near the dome surface rather than bubble formation and collapse within the conduit. In such a case, the temporal occurrence pattern of families may be relatively simple, as represented by TYPE II in Section 4.2. We consider that the difference between HF and LF events that can be explained by the double-couple force is related to the stiffness of rock in the source area. In general,

however, most LF events are considered to result from fluid-pressurization processes (e.g., Chouet, 1992; McNutt, 1996). Accordingly, we consider that the source mechanism of LF events described above is also one of the source processes for summit LF events. The fact that a number of LF events were accompanied by weak gas emission from the dome surface (Yamasato, 1998) is evidence that the occurrence of LF events is related to the activity of fluids. Goto (1999) demonstrated that the brittle failure of melt is a candidate process for the generation of earthquakes within the summit area. As the hypocenters of LF events are widely distributed above 500 m ASL, several different types of source processes should be considered in further studies.

## **6. Conclusions**

The present study describes the temporal characteristics of summit seismicity over the period from immediately prior to dome emergence until the cessation of dome growth. The temporal characteristics of seismicity levels were different for exogenous and endogenous periods of dome growth. Periods of solely exogenous growth were accompanied by several days or weeks of increased seismicity, while levels of seismicity were notably low between successive seismically active periods. In contrast, periods of endogenous growth were accompanied by high levels of seismicity, with repeated cycles of increasing and decreasing seismicity over periods of one to two months. The dominant waveform types recorded over the period of dome growth changed sequentially from LF to HF and MF types, except that HF events increased in intensity during May 1991. HF and MF events are mainly distributed at depths of 500–1100 m ASL, just below the lava dome, while LF events are widely distributed at depths from 500 m ASL to the interior of lava dome itself. We observed a large number of earthquake families during the study period. The duration of most families was less than two weeks and was not related to the intensity of their activity. The incidence rate

of events in each family culminated in the middle of the respective activity periods, and the waveforms of several analyzed families evolved gradually over time. At times of intensified HF events, several families appeared contemporaneously, whereas at times of intensified LF events, the occurrence pattern of families was relatively simple: a new family only began to activate once the activity of the previous family had declined or ceased completely. A possible source mechanism for families of HF events is stick-slip within the stiff rocks surrounding the conduit; however, several different types of source mechanisms should be considered for families of LF events.

### **Acknowledgments**

This work was partly supported by the Unzen Scientific Drilling Project (USDP) funded by the Ministry of Education, Culture, Sports, Science and Technology, Japan. We thank V.M. Zobin and an anonymous reviewer for their helpful comments and suggestions that significantly improved the manuscript.

### **References**

- Chouet, B.A., 1992. A seismic model for the source of long-period events and harmonic tremor. In: Gasparini, P., Scarpa, R., Aki, K. (Eds.). *Volcanic Seismology*. IAVCEI Proceedings in Volcanology, Springer-Verlag, Berlin, pp. 133–156.
- Geophysical Party, Joint University Research Group, 1992. Geophysical observation of the 1990–1992 eruption at Unzen Volcano (Part 1), *Bull. Volcanol. Soc. Japan*, 37, 209–215, in Japanese.
- Goto, A., 1999. A new model for volcanic earthquake at Unzen Volcano: melt rupture model. *Geophys. Res. Lett.* 26 (16), 2541–2544.
- Green, D.N, Neuberg, J., 2006. Waveform classification of volcanic low-frequency earthquake swarms and its implication at Soufriere Hills Volcano, Montserrat. *J.*

- Volcanol. Geotherm. Res. 153, 51–63.
- Japan Meteorological Agency, 2002. Report on the eruption of the Unzen Volcano, 1991. Technical report of the Japan Meteorological Agency, No.123, 372 pp., in Japanese.
- McNutt, S.R., 1996. Seismic monitoring and eruption forecasting of volcanoes: a review of the state-of-the-art and case histories. In: Scarpa, R., Tilling, R. (Eds.), *Monitoring and Mitigation of Volcano Hazards*. Springer, Berlin, pp. 99–146.
- Mizukoshi, I., Moriya, T., 1980. Broad band and wide dynamic range observation of Usu Volcano earthquake swarm. *J. Seismol. Soc. Jpn.* 33, 479–491. in Japanese.
- Nakada, S., Shimizu, H., Ohta, K., 1999. Overview of the 1990–1995 eruption at Unzen Volcano. *J. Volcanol. Geotherm. Res.* 89, 1–22.
- Ohta, K., 1997. Reviews on the prediction of the 1990–1995 eruption of Unzen Volcano and supporting system for risk management. *Bull. Volcanol. Soc. Jpn.* 42, 61–74, in Japanese.
- Okada, H., Watanabe, H., Yamashita, H., Yokoyama, I., 1981. Seismological significance of the 1977–1978 eruptions and the magma intrusion process of Usu Volcano, Hokkaido. *J. Volcanol. Geotherm. Res.* 9, 311–334.
- Power, J.A., Lahr, J.C., Page, R.A., Chouet, B.A., Stephens, C.D., Harlow, D.H., Murray, T.L., Davies, J.N., 1994. Seismic evolution of the 1989–1990 eruption sequence of Redoubt Volcano, Alaska. *J. Volcanol. Geotherm. Res.* 62, 69–94.
- Saito, E., Suto, S., Soya, S., Kazahaya, K., Kawanabe, Y., Hoshizumi, H., Watanabe, K., Endo, H., 1993. Geodetic monitoring using EDM before and during the 1991–1992 lava extrusion of Fugen-dake, Unzen Volcano, Kyushu, Japan. *Bull. Geol. Surv. Japan.*, 44 (10), 639–647, in Japanese.
- Shimizu, H., Matsuwo, N., Umakoshi, K., 1994. Magma ascent process at the shallow part of conduit of Unzen Volcano: information from seismic activities. *Abstr., Volcanol. Soc. Jpn.* 2, p.97, in Japanese.

- Shimizu, H., Matsuwo, N., Umakoshi, K., Matsushima, T., 1992a. Seismic activity beneath the lava domes of Unzen Volcano. *Abstr., Volcanol. Soc. Jpn.* 2, p.17, in Japanese.
- Shimizu, H., Umakoshi, K., Matsuwo, N., Ohta, K., 1992b. Seismological observations of Unzen Volcano before and during the 1990–1992 eruption, In: Yanagi, T., Okada, H., Ohta, K. (Eds.), *Unzen Volcano, The 1990–1992 Eruption*. The Nishinippon and Kyushu University Press, pp. 38–43.
- Shimizu, H., Umakoshi, K., Matsuwo, N., Matsushima, T., Ohta, K., 1997. Seismic activity associated with the magma ascent and dome growth of Unzen Volcano. *Unzen international workshop: decade volcano and scientific drilling, Proceedings*, pp. 42–44.
- Stephens, C.D, Chouet, B.A., 2001. Evolution of the December 14, 1989 precursory long-period event swarm at Redoubt Volcano, Alaska. *J. Volcanol. Geotherm. Res.* 109, 133–148.
- Sudo, Y., Tsutsui, T., Sako, M., Masuda, H., Hoka, T., Yamada, T., 1992. Seismic observation at Nodake, Unzen Volcano. In: Ohta, K.(Ed.), *Research on the prediction of lava extrusion at Unzen Volcano*, *Sci. Rep. Grant-in-Aid from Ministry of Education*, pp.21–28, in Japanese.
- Sudo, Y., Sako, M., Masuda, H., Hoka, T., Yamada, T., Yoshikawa, S., Tsutsui, T., 1994. Seismic observation at Nodake, Unzen Volcano (2). In: Ohta, K.(Ed.), *Research on the formation and the collapses of lava dome at Unzen Volcano*, *Sci. Rep. Grant-in-Aid from Ministry of Education*, pp.23–37, in Japanese.
- Suto, S., Saito, E., Yasuda, A., Soya, T., Kazahaya, K., Kawanabe, Y., 1994. Ground deformation at the summit area of Unzen volcano since November in 1993, *Abstr. Jpn. Earth & Planetary Sci. Joint Meeting*, p.98, in Japanese.
- Umakoshi, K., Shimizu, H., Matsuwo, N., 2001. Volcano-tectonic seismicity at Unzen

- Volcano, Japan, 1985–1999. *J. Volcanol. Geotherm. Res.* 112, 117–131.
- Umakoshi, K., Shimizu, H., Matsuwo, N., 2002. Seismic activity associated with the growth of the lava dome at Unzen Volcano (November 1993-January 1994) –grouping of earthquakes on the basis of cross-correlations among their waveforms–. *Bull. Volcanol. Soc. Jpn.* 47, 43–55, in Japanese.
- Urabe, T., Umakoshi, K., Shinohara, M., Ohmi, S., Takahama, S., Kochi, N., Sato, H., Suzuki, T., Kaiho, Y., Asanuma, T., Suyehiro, K., Nishizawa, A., 1987. Crustal structure beneath the Shimabara Peninsula by air-gun experiment. *Abstr. Ann. Meet. Seismol. Soc. Jpn.*, No. 1, p.332, in Japanese.
- White, R.A., Miller, A.D., Lynch, L., Power, J., 1998. Observations of hybrid seismic events at Soufriere Hills Volcano, Montserrat: July 1995 to September 1996. *Geophys. Res. Lett.* 25, 3657–3660.
- Yamasato, H., 1998. Nature of infrasonic pulse accompanying low frequency earthquake at Unzen Volcano, Japan. *Bull. Volcanol. Soc. Jpn.* 43, 1–13,
- Yamashina, K., Matsushima, T., Ohmi, S., 1999, Volcanic deformation at Unzen, Japan, visualized by a time-differential stereoscopy. *J. Volcanol. Geotherm. Res.* 89, 73–80.
- Zobin, V.M., Orozco-Rojas, J., Reyes-Davila, G.A., Navarro, C., 2005. Seismicity of an andesitic volcano during block-lava effusion: Volcan de Colima, Mexico, Noveber 1998– January 1999. *Bull. Volcanol.* 67, 679–688

## Figure Captions

Table 1

Periods of each sub-stage determined in this study and the number of events and percentages of each waveform type.

Fig. 1. (a) Location map of Unzen Volcano, Japan. (b) Hypocentral distribution of VT earthquakes during the period 1989–1995 (Umakoshi et al., 2001). (c) Hypocentral distribution of summit earthquakes during the period May 1991 to February 1995, as determined by SEVO. The planar termination of hypocenters at the altitude of 1300 m is due to a constraint of the computations. E-W cross-sections of topography before and after dome extrusion are delineated by dashed and solid lines, respectively. The change in elevation to the east of the dome is due to deposits derived from pyroclastic flows. The solid triangle marks the summit of Fugendake.

Fig. 2. Temporal changes in the effusion rate of lava during the period 1991–1995 (Nakada et al., 1999). Stages 1, 2 and 3 defined at the top of the figure, which were proposed by Ohta (1997) based on the dominant growth style of the lava dome, were added by the authors.

Fig. 3. Locations of seismograph stations in the area close to the lava dome. These stations were installed prior to dome (Lobe 1) extrusion on May 20, 1991. Note that FG3 was moved to a new location at FG4 during June 1993. The previous Jigokuato crater, from where Lobe 1 extruded, is located immediately beneath the peak of Heisei-Shinzan. The topographic base map used in the figure was published by the Geographical Survey Institute of Japan in 2004. Intervals for thick contour lines are 25 m.

Fig. 4. Examples of waveforms and normalized spectra for HF, MF, and LF event types. Spectra were calculated by FFT with a window length of 5.12 s from 0.5 s before onset.

Fig. 5. (a) Temporal variations in the growth style of the lava dome. Black and white rectangles indicate exogenous and endogenous periods of growth of the lava dome, respectively. The period when a lava spine was upheaving is shown by a grey rectangle. Vertical numbered bars indicate the dates of the appearances of new lobes. (b) Three stages of dome growth (Ohta, 1997) and sub-stages determined in the present study based on temporal characteristics of seismicity and waveform types. (c) Daily number of summit earthquakes with maximum amplitudes equal to or more than  $1 \times 10^{-3}$  cm/s, as recorded at seismic stations FG3 and FG4. The lengths of red, green, and blue bars correspond to the numbers of HF, MF, and LF events, respectively. (d) Number of events with a peak cross-correlation coefficient (PCC) equal to or greater than 0.6 within 24 h either side of each reference event. The horizontal axis is the occurrence time of reference events.

Fig. 6. Results of cross-correlation analysis for the period May 15 to June 15, 1994. The vertical axis represents the number of events with PCCs equal to or more than a given threshold value within 24 h either side of the reference event. The horizontal axis is the occurrence time of reference events. Figs. (a) to (f) were compiled using different threshold values.

Fig. 7. Examples of waveforms recorded during each month, as represented by events with the highest peaks in Fig. 5(d). Waveforms are normalized to the relevant

maximum amplitude. The upper-left and bottom-left numbers for each waveform indicate the month/day, and the peak values in Fig. 5(d) and the duration of the family (days), respectively. In the case of ambiguous base widths of arch-like distribution of data in Fig. 5(d), the duration could not be measured, and is indicated by “-”.

Fig. 8. Enlargement of part of Fig. 5(d) for (a) May 11–31, 1991; (b) May 15 to June 4 1994; (c) December 1–21, 1991; and (d) July 24 to August 13, 1993. Two occurrence patterns of families (TYPE I, TYPE II) defined in this study are indicated at the upper-left in each diagram. Families F1–F4 are indicated by red dots and are discussed in Section 5.

Fig. 9. Hypocentral distribution of HF, MF, and LF events obtained by classifying the events shown in Fig. 1(c).

Fig. 10. Locations of seismograph stations used for the hypocentral determination of summit earthquakes by SEVO (Shimizu et al., 1994). Six stations—FG1, FG2, FG3 or FG4 (see Fig. 3), TKE, KRA or KRE, and FKE or YTE—were always used in locating hypocenters. Contour intervals are 200 m.

Fig. 11. Data for families F1–F4. (a) PCCs between the master event and all extracted events. (b) Number of events within 3-hour intervals. (c) Maximum amplitude measured in digital counts.

Table 1

Stage	Period	HF	%	MF	%	LF	%	Total
1-1	May 1991	18759	58	5588	17	7774	24	32121
1-2	Jun. 1–Nov. 23, 1991	1263	3	4958	11	38987	86	45208
1-3	Nov. 24, 1991–Dec. 31, 1992	1402	1	12951	7	164568	92	178921
2-1	Jan. 1–Aug. 31, 1993	2361	2	6957	6	101411	92	110729
2-2	Sep. 1–Nov. 18, 1993	1853	7	14777	55	10262	38	26892
3-1	Nov. 19, 1993–Sep. 30, 1994	95847	52	62008	33	27810	15	185665
3-2	Oct. 1, 1994–Feb. 28, 1995	1190	38	629	20	1337	42	3156
Total		122675	21	107868	19	352149	60	582692

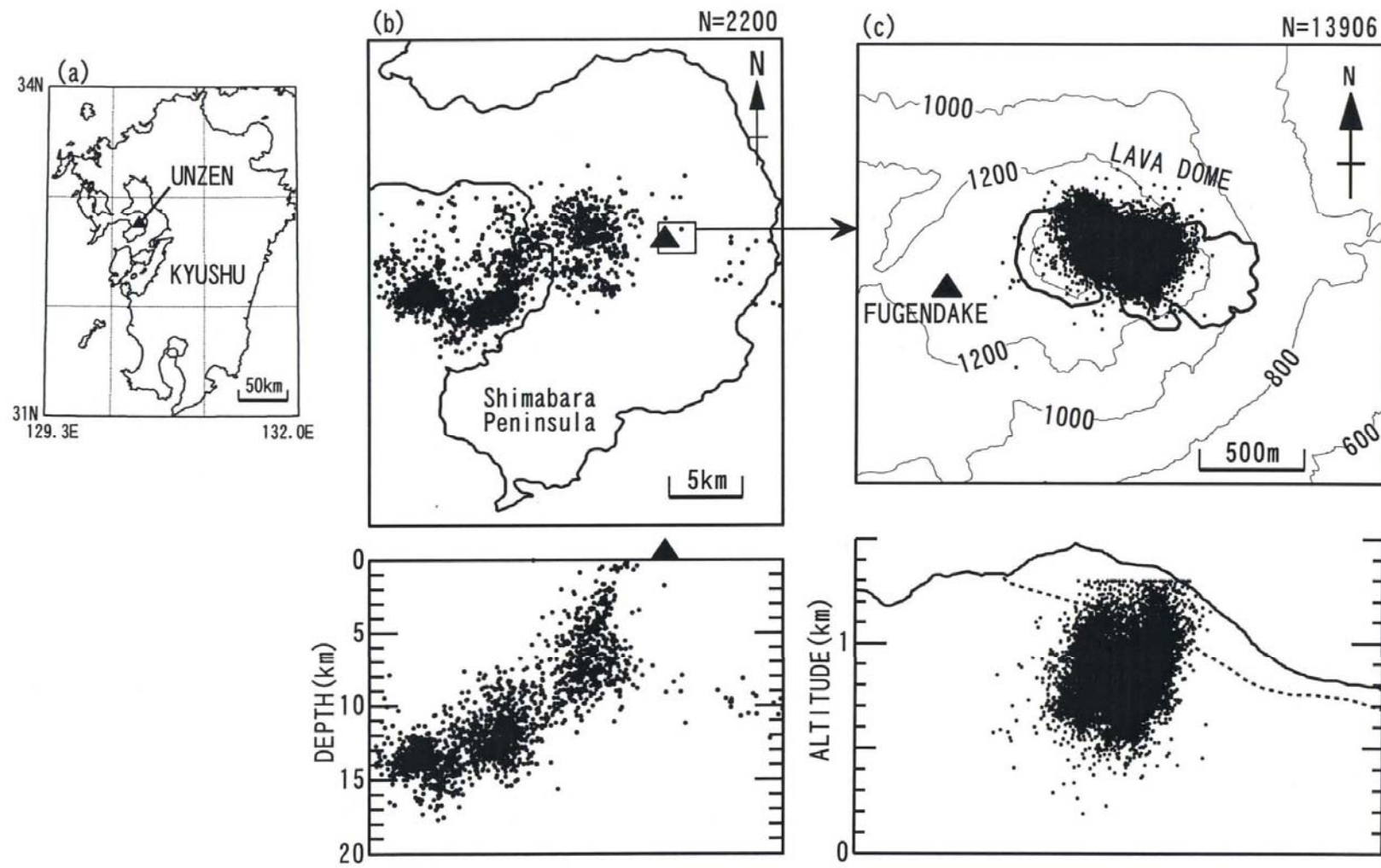


Figure 1



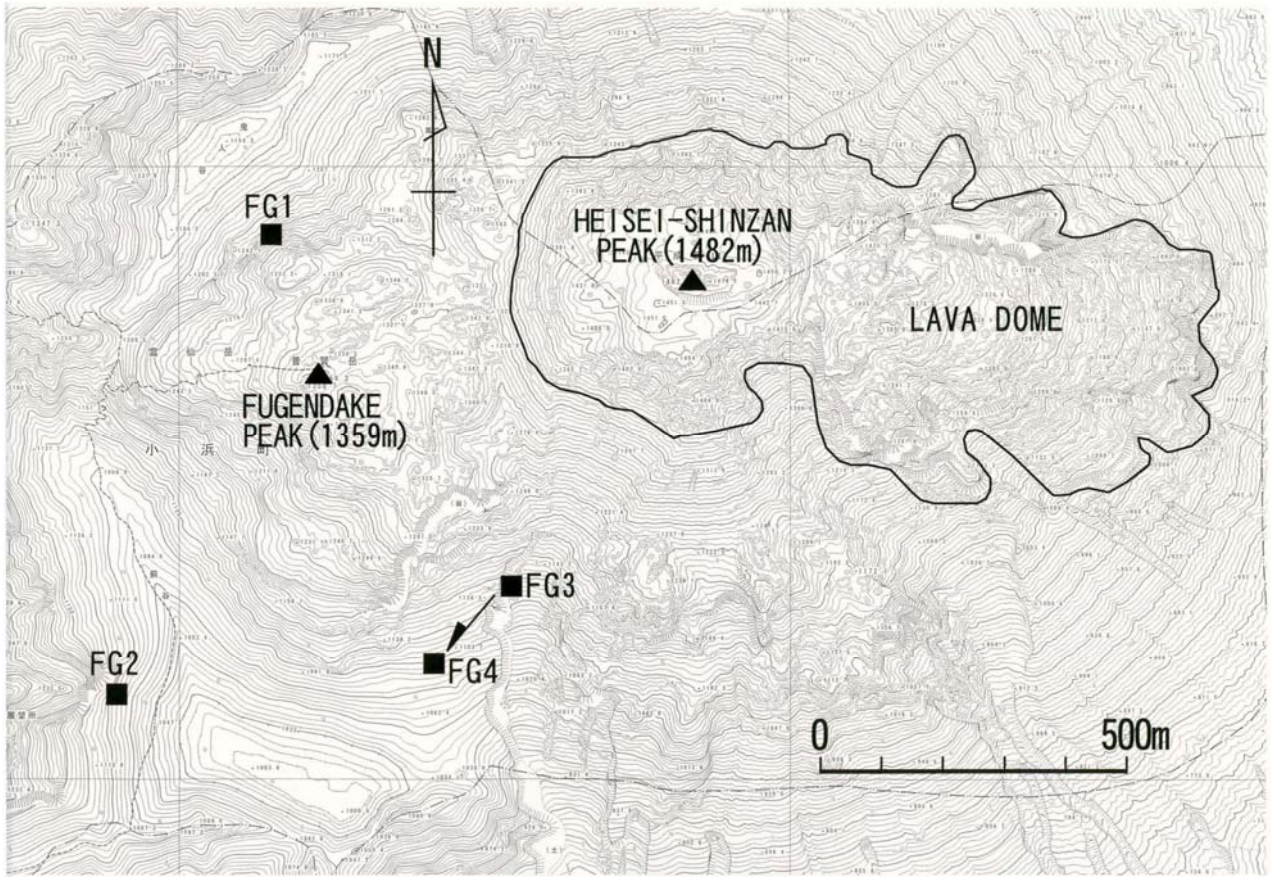


Figure 3

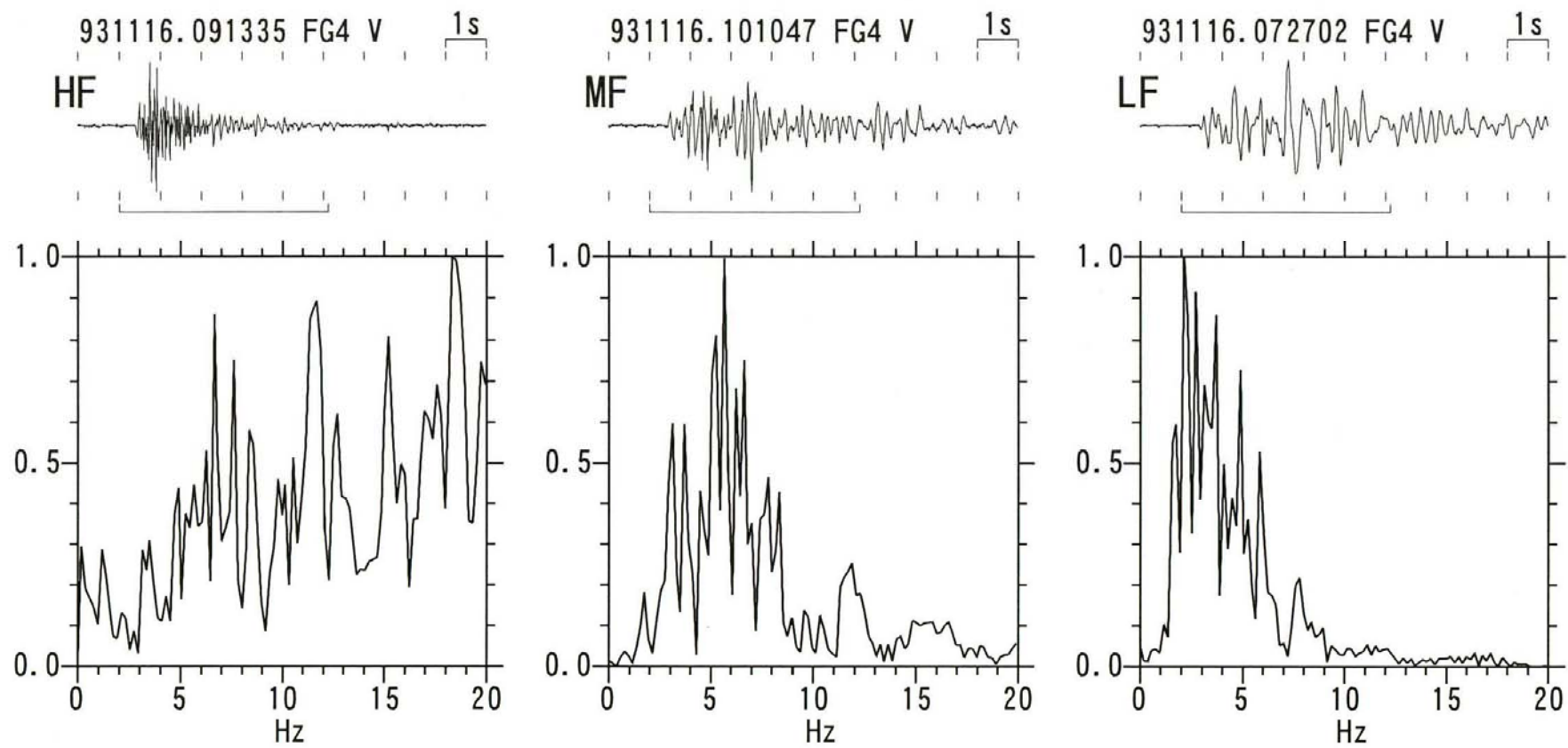


Figure 4

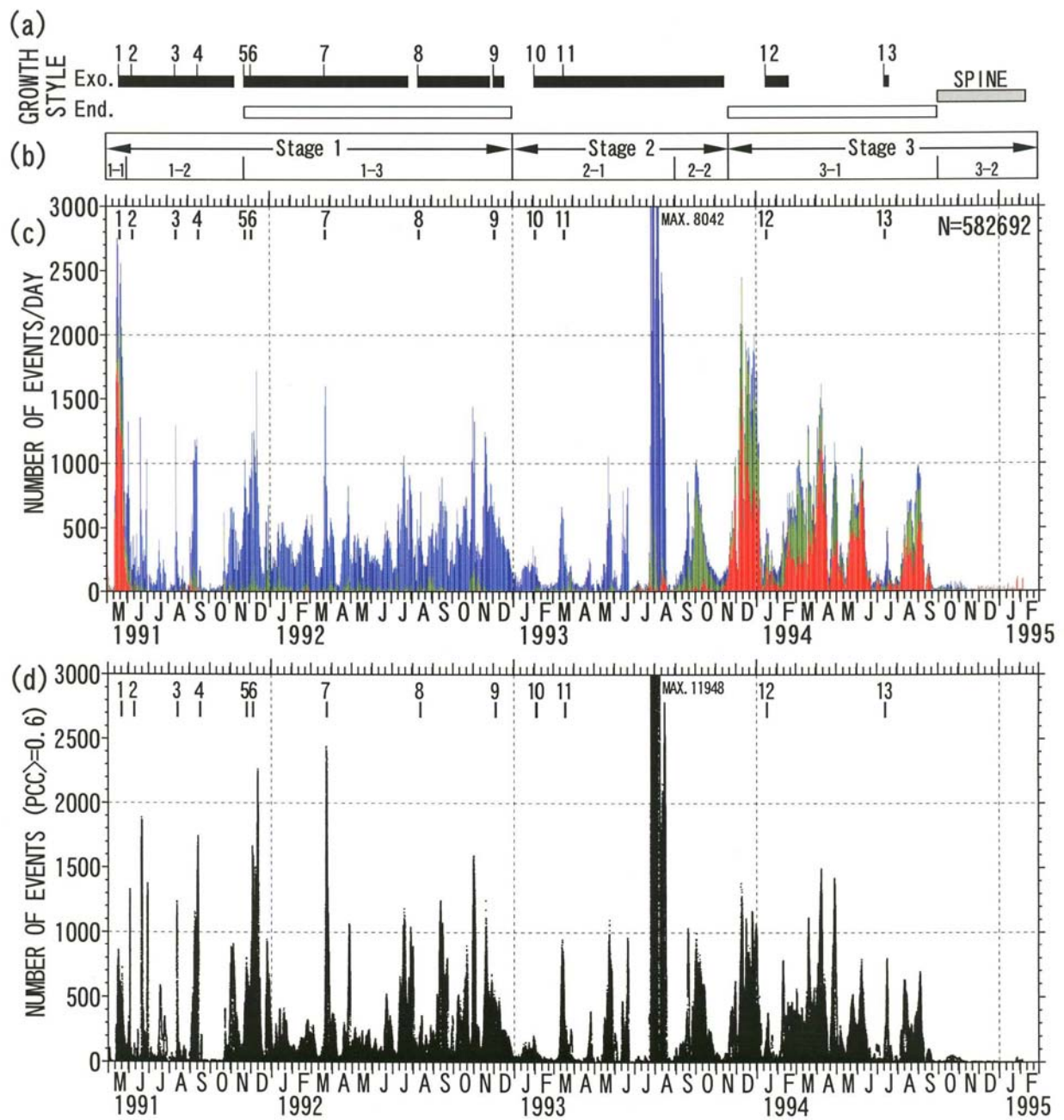


Figure 5

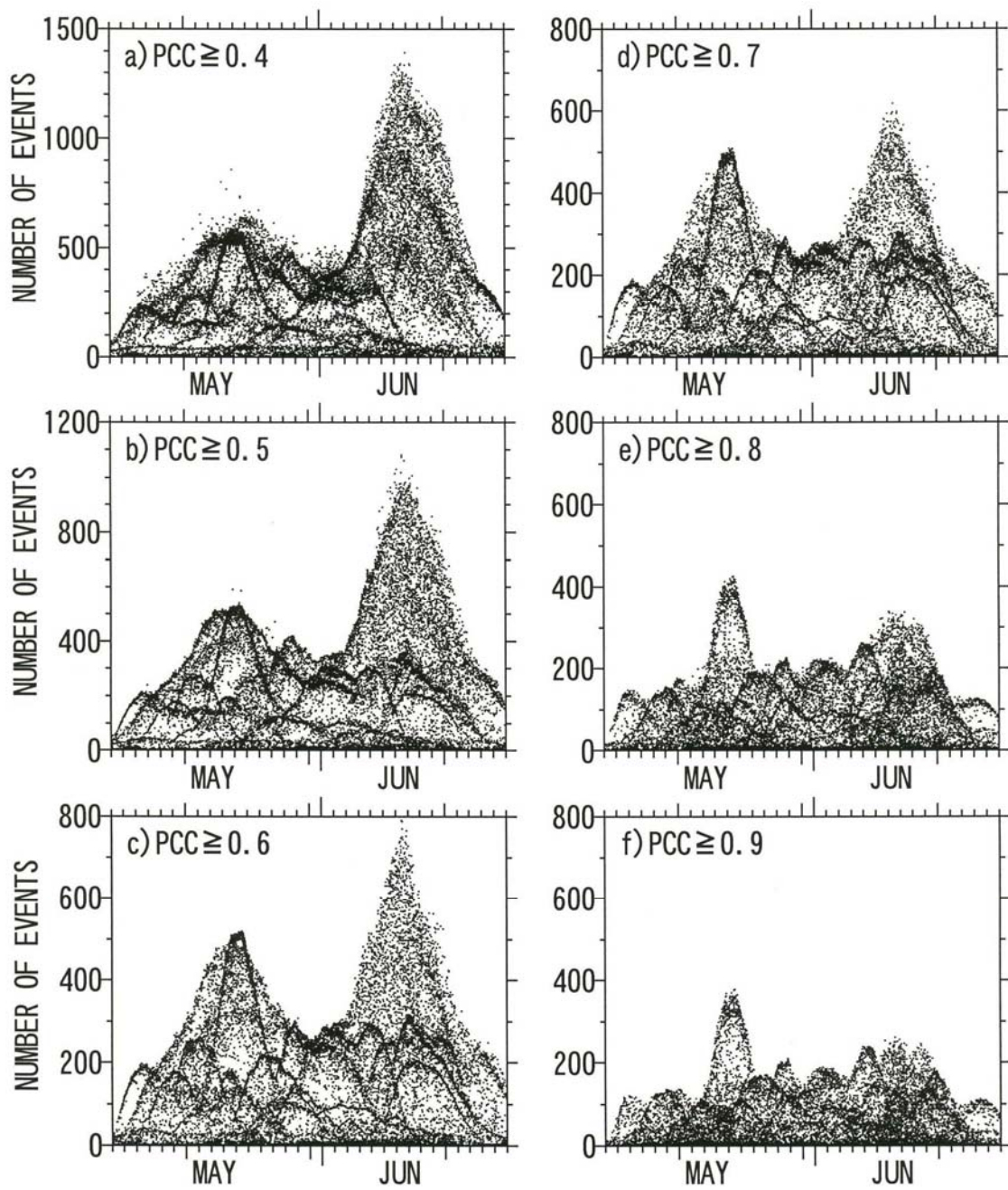


Figure 6

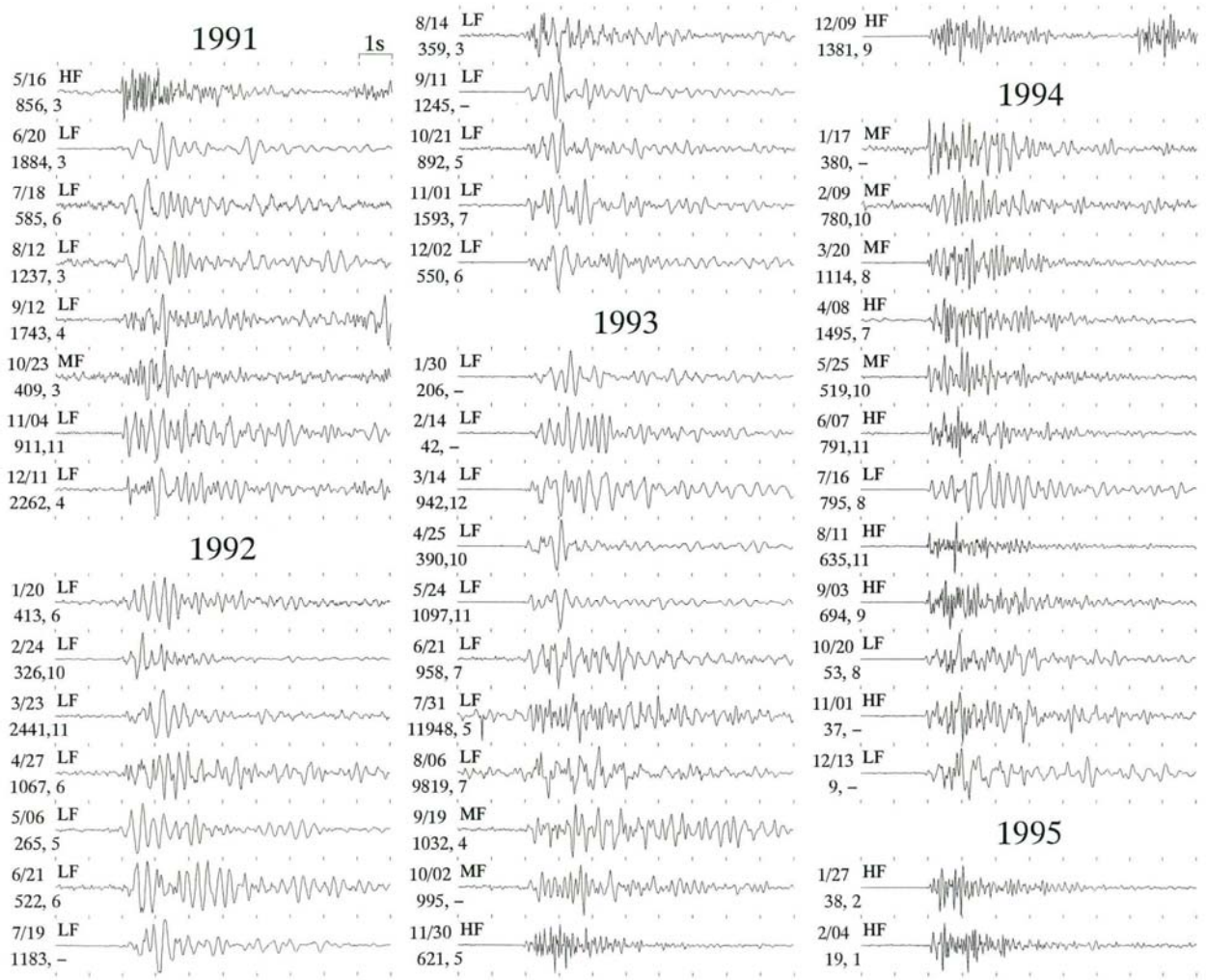


Figure 7

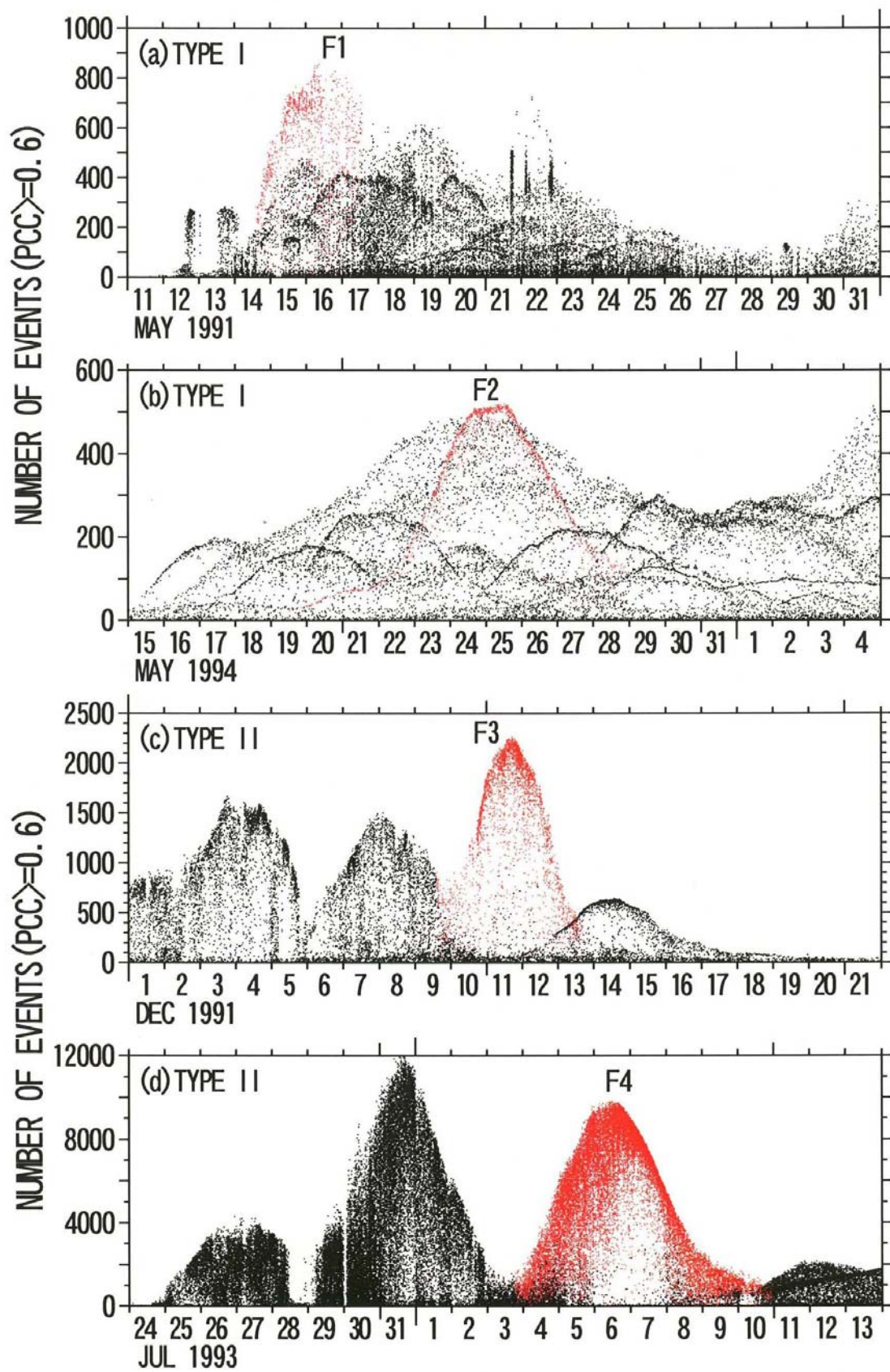


Figure 8

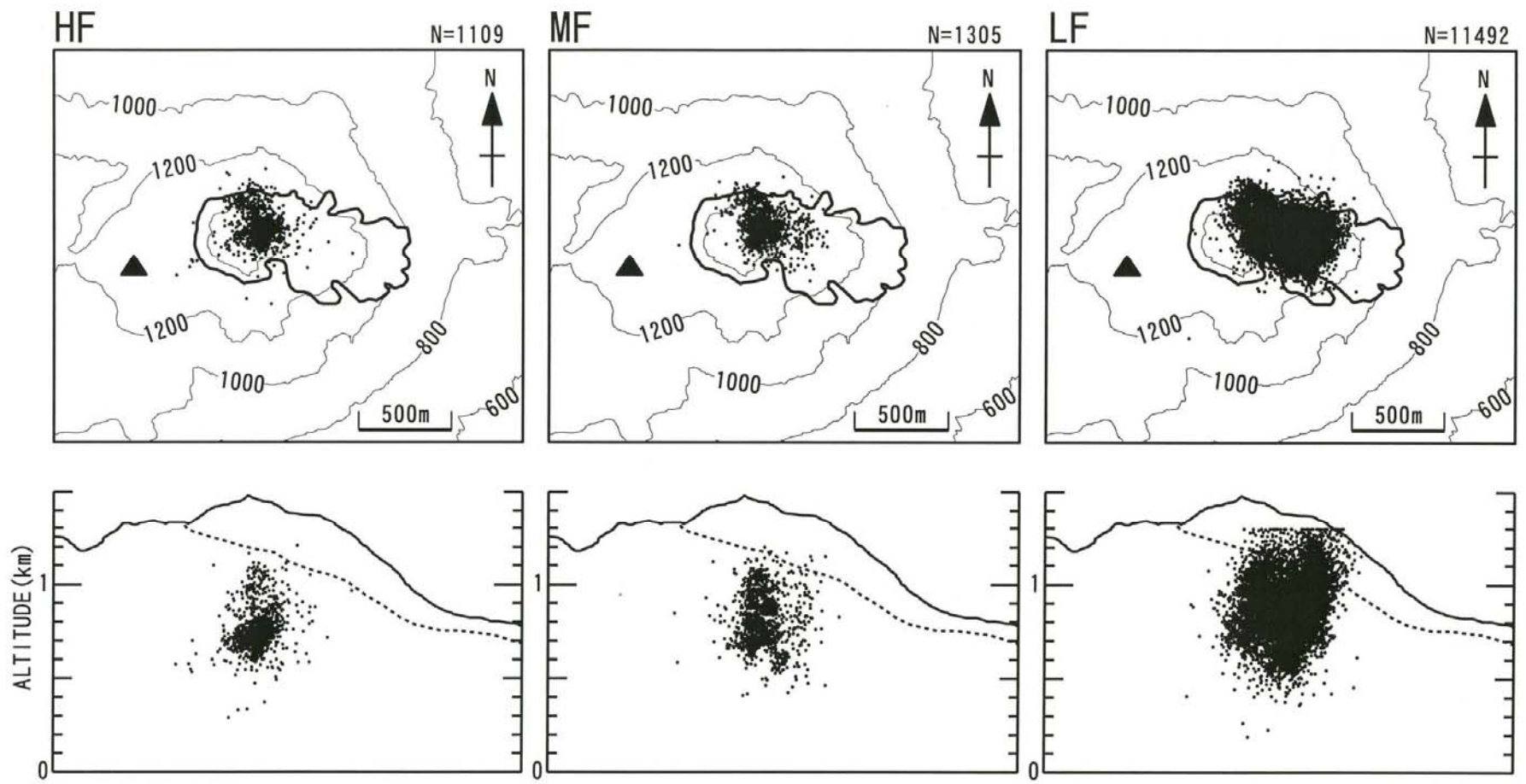


Figure 9

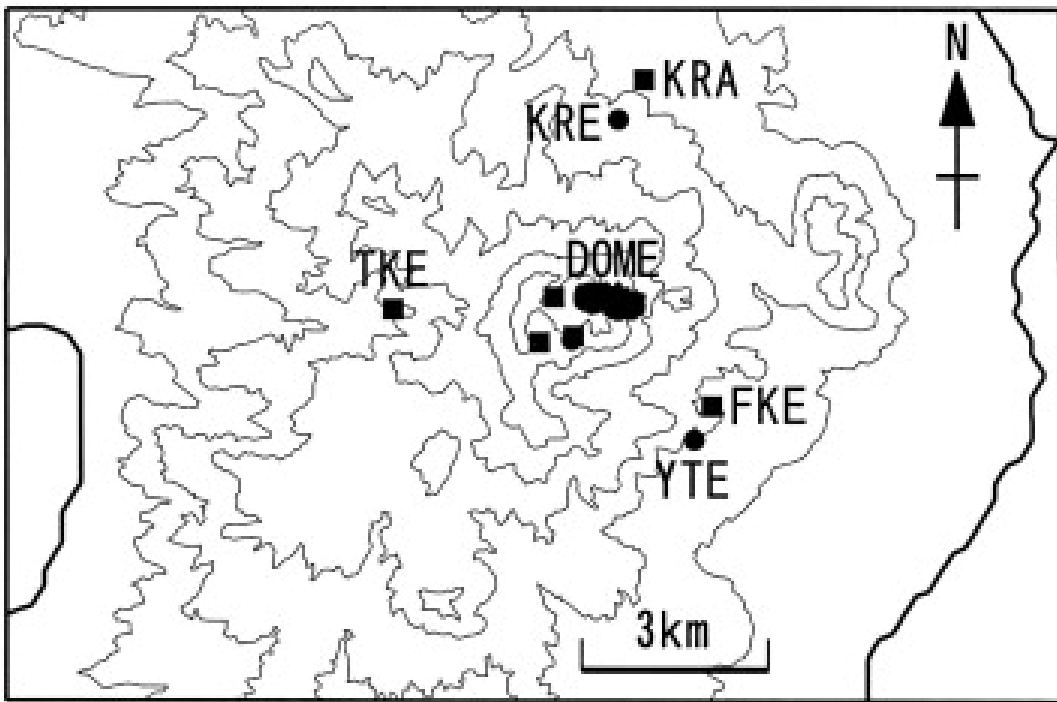


Figure 10

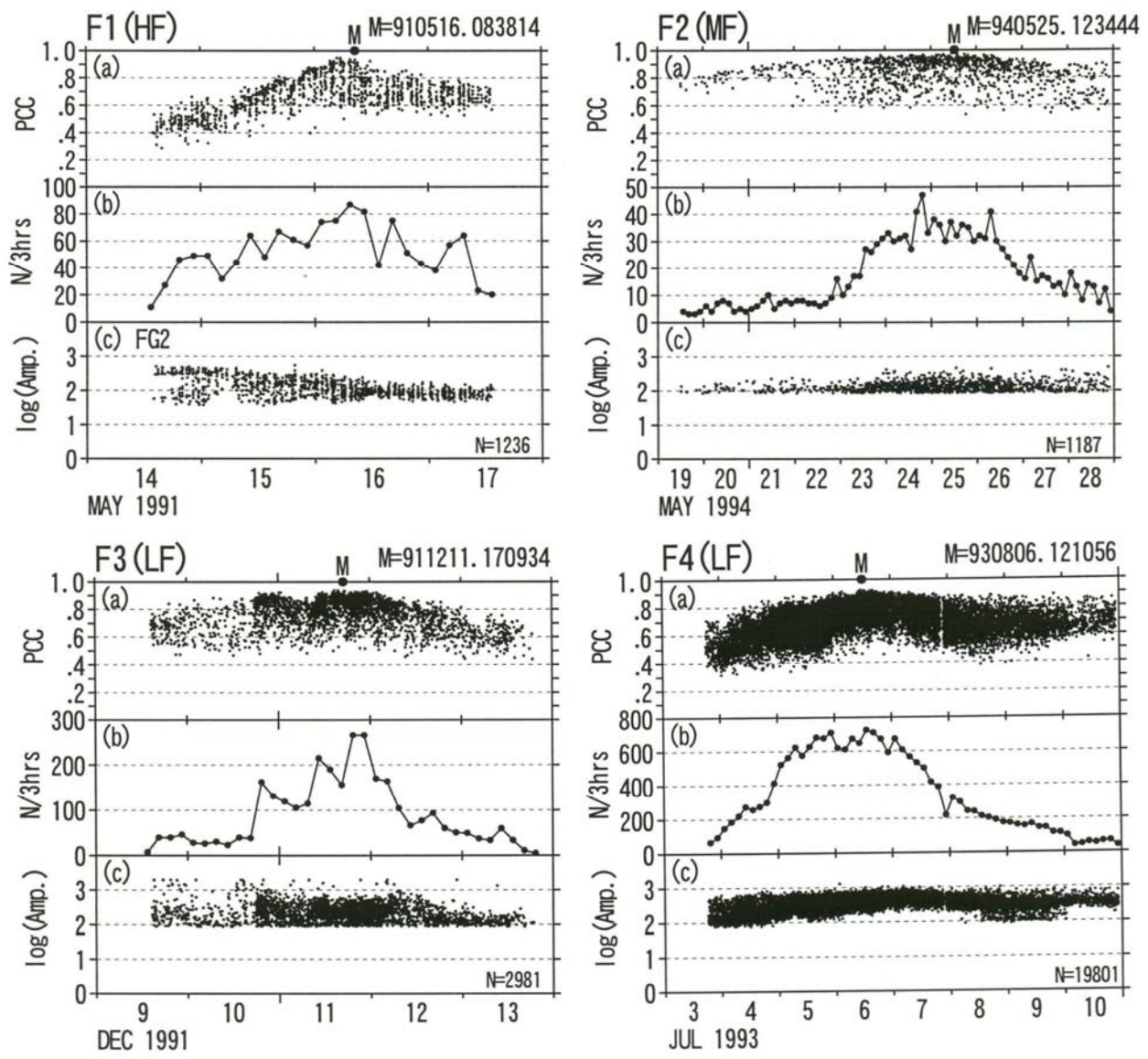


Figure 11